

A wireless guided wave excitation technique based on laser and optoelectronics

Hyun-Jun Park¹, Hoon Sohn^{1*}, Chung-Bang Yun¹, Joseph Chung² and Il-Bum Kwon³

¹Department of Civil and Environmental Engineering, Korea Advanced Institute of Science and Technology, Guseong-dong, Yuseong-gu, Daejeon, Korea

²Senior Manager, R&D Department, CyTronIQ Co. Ltd., Hoseo University, Sechul-ri, Baebang-myun, Asan, Korea

³Center for Safety Measurement, Korea Research Institute of Standards and Science, Doryong-dong, Yuseong-gu, Daejeon, Korea

(Received November 18, 2009, Accepted February 11, 2010)

Abstract. There are on-going efforts to utilize guided waves for structural damage detection. Active sensing devices such as lead zirconate titanate (PZT) have been widely used for guided wave generation and sensing. In addition, there has been increasing interest in adopting wireless sensing to structural health monitoring (SHM) applications. One of major challenges in wireless SHM is to secure power necessary to operate the wireless sensors. However, because active sensing devices demand relatively high electric power compared to conventional passive sensors such as accelerometers and strain gauges, existing battery technologies may not be suitable for long-term operation of the active sensing devices. To tackle this problem, a new wireless power transmission paradigm has been developed in this study. The proposed technique wirelessly transmits power necessary for PZT-based guided wave generation using laser and optoelectronic devices. First, a desired waveform is generated and the intensity of the laser source is modulated accordingly using an electro-optic modulator (EOM). Next, the modulated laser is wirelessly transmitted to a photodiode connected to a PZT. Then, the photodiode converts the transmitted light into an electric signal and excites the PZT to generate guided waves on the structure where the PZT is attached to. Finally, the corresponding response from the sensing PZT is measured. The feasibility of the proposed method for wireless guided wave generation has been experimentally demonstrated.

Keywords: wireless power transmission; laser; optoelectronics; active sensing; guided wave generation.

1. Introduction

In recent years, guided wave based structural health monitoring (SHM) techniques have attracted much attentions, because they are not only sensitive to small defects but also capable to propagate over a long distance in plate and pipe like structures. A number of studies have demonstrated the potential of guided wave based SHM (Moulin *et al.* 1997, Sohn 2003, Sohn *et al.* 2004, Kim and Sohn 2007, Raghavan and Cesnik 2007, Wang and Yuan 2007, Giurgiutiu 2008).

Guided waves can be generated in a structure using various devices such as ultrasonic probes, piezoelectric elements and lasers. Ultrasonic probes include wedge-coupled (Guo and Cawley 1994), air-coupled (Castaings and Hosten 2001), fluid-coupled (Ghosh *et al.* 1998), and electro-magnetic

*Corresponding Author, Associate Professor, E-mail: hoonsohn@kaist.ac.kr

acoustic transducers (EMATs) (Guo *et al.* 1997). However, these probes can have low sensitivity due to the acoustic impedance mismatch between air/fluid couplants and the objects. EMATs have restrictions on the applicable frequency range, and they require electrical conductivity of the objects (Achenbach 2000).

Piezoelectric lead zirconate titanate (PZT) elements could be a good candidate for such online applications due to its small size, easy installation, low cost, nonintrusive nature, and wide frequency response range. PZT transducers typically require wires to supply the power necessary for generation of guided waves and to transmit the sensed data, but the installation of wires in real structures can be expensive and labor-intensive (Çelebi 2002). To overcome these problems, there are on-going efforts to integrate a PZT transducer with a wireless sensor unit (Lynch and Loh 2006, Mascarenas *et al.* 2007, Grisso and Inman 2008, Lu *et al.* 2008). One of major challenges in such wireless systems is to secure power necessary to operate the wireless sensors. However, because guided wave based active sensing devices demand relatively high electric power compared to conventional passive sensors such as accelerometers and strain gauges (Yeatman 2009), existing battery technologies may not be suitable for long-term operation of active sensing devices.

Laser-based excitation techniques can be an alternative. Electromagnetic radiation from a laser is absorbed in the surface region of a structure, causing heating. The heated region undergoes thermal expansion, and non-contact guided waves are generated (Scruby and Drain 1990). However, in the current laser technique, it is difficult controlling the excitation source to generate desired arbitrary waveforms. Other researchers attempted to generate narrow-band guided waves using a laser (Clark *et al.* 1998) but were able to control only the frequency content of the generated waves not the actual waveform.

The ultimate goal of our research is to develop an optical system for guided wave generation and sensing. This paper mainly focuses on the excitation aspect of the overall system. The proposed wireless technique transmits power necessary for PZT excitation using laser and optoelectronic devices. Because power is remotely transmitted to the PZT transducer, no complex electronic components are necessary at the PZT node, making it possible to develop a self-contained, rugged, and non-intrusive PZT node. The transducer itself can be entirely passive and consequently will have a long lifetime when it has rugged packaging. In addition, any arbitrary waveform can be generated by a laser using an electro-optic modulator (EOM). This wireless power transmission scheme also can be expanded to transmit power through optical fibers and generate guided waves (Lee *et al.* 2009). A further research for wireless guided wave sensing is currently being developed by the authors using other optoelectronic devices, such as photovoltaic panels and laser diodes (Park *et al.* 2010). Finally, as shown in Fig. 1, it is envisioned that the develop technology can be integrated with autonomous

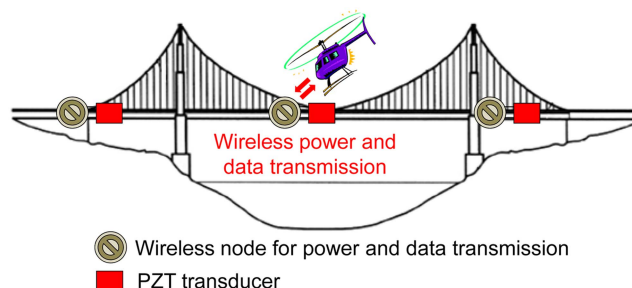


Fig. 1 Integration optics-based active sensing technology and remote platforms based on unmanned autonomous inspection robot for civil application

moving agents such as robots to remotely inspect the integrity and performance of large distributed infrastructure systems such as bridges.

This paper is organized as follows. First, the operational principle of the proposed system is described. Electrical circuit analysis and experimental tests are then executed to investigate the feasibility of the proposed technique, and the results are discussed. Finally, the paper concludes with a summary and future work.

2. Principle of operation

Fig. 2 shows an overall schematic of the proposed wireless guided wave excitation and sensing system. It takes advantage of optical techniques for both guided wave generation and sensing. First, a laser wirelessly transmits a generated waveform to a PZT transducer node that consists of a photodiode, a transformer and a PZT transducer. Then, the photodiode converts the light into an electric signal, and the transformer increases the voltage level of the created electric signal. The electric input signal excites the PZT attached on a structure, and the excited PZT consequently creates guided waves within the structure. Next, the corresponding reflected waves are measured by the identical PZT and re-converted into a laser and transmitted back to another photodiode located in the data acquisition unit for diagnosis. This paper mainly focuses on the wireless guided wave generation aspect of the overall system.

There are critical components necessary for wireless excitation of a PZT transducer in the proposed system; a laser as a power source, an electro-optic modulator for modulation of the laser intensity, an arbitrary waveform generator for generating a waveform such as a toneburst signal, an optical amplifier for optical power amplification, a photodiode for conversion of light into an electric signal, a transformer for voltage amplification, and a PZT transducer for guided wave generation. In the following subsections, the operational principle for each component will be briefly discussed.

2.1 Laser as a wireless power transmission source

Lasers can be characterized by a number of key optical properties, and these properties dictate

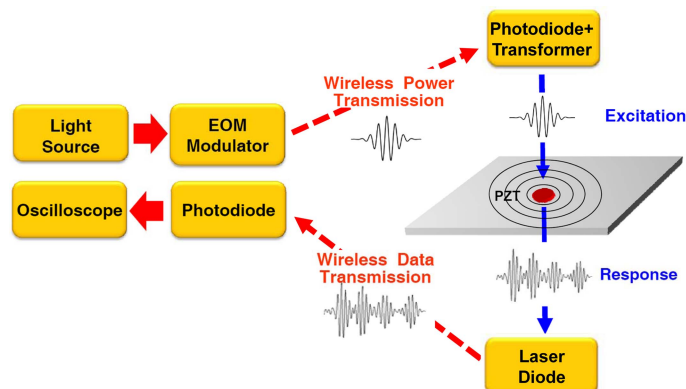


Fig. 2 An overall schematic for optics based wireless guided wave generation and sensing

which lasers are suitable for wireless power transmission. The most unique property of the laser is its directionality. The laser emits highly directional and collimated radiation with a low angle of divergence (Svelto 1982). This is essential for wireless power transmission because the energy carried by the laser beam can be transmitted for a long distance and focused onto a small area. On the other hand, the radiation of conventional lights spreads out in all directions. Although conventional lights can be focused onto a small area using a focal lens, the energy density is very low. It is because that the conventional lights have numerous wavelength components and each component has its own refraction ratio. Therefore, only a small portion of the conventional lights can be focused onto a target area and efficiency of energy transmission drastically decreases. One final concern when using a laser is laser safety. Generally, a laser with over 10 mW is required for wireless power transmission. In this case, the laser source is classified as *Class 3B* based on standards such as BS4803 in Europe or ANSI Z136 in US. Accordingly direct beam viewing could be hazardous, and the use of the laser requires caution for user safety.

2.2 Generation of an arbitrary waveform using an electro-optic modulator

To remotely excite a PZT transducer with an arbitrary waveform, the modulation of the laser intensity is necessary. This modulation can be achieved using an EOM. The EOM is an optical device in which the electro-optic effect is used to modulate the intensity of light. When an external electric field is applied to a crystal, such as lithium niobate (LiNbO₃), in the EOM, the polarizability and the refractive index of the crystal change in response to the applied electric field (Smith 1995). This results in the transmission rate change of light intensity passing through the EOM as

$$Tr(\%) = \sin^2\left(\frac{\pi V}{2V_\pi}\right) \quad (1)$$

Here Tr , V and V_π are the transmission rate, the applied electric voltage, and the voltage required for maximum transmission of the laser intensity, respectively.

Considering the relationship between the transmitted intensity (amplitude) of the laser versus the applied voltage, it is obvious that the transmitted intensity is a nonlinear function of the applied voltage ($Tr \sim \sin^2 V$). Local linear modulation can be performed by modulating the light intensity

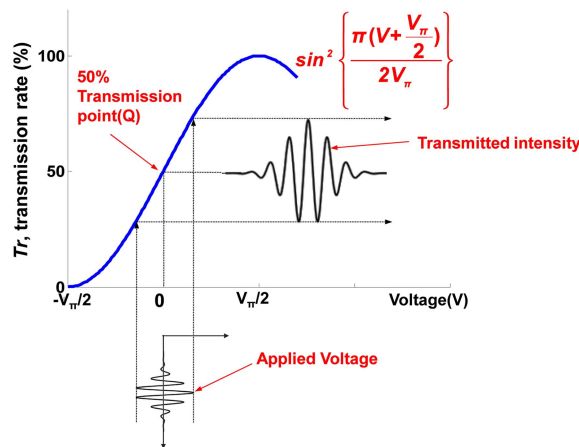


Fig. 3 Local linear modulation of the laser intensity near the 50% transmission point (Q) of the EOM

near the 50% transmission point, Q in Fig. 3, of the modulator rather than the origin. To achieve this, a quarter-wave plate (Khare 2004) is added to the EOM. This plate introduces a phase shift of $V_{\pi}/2$ and forces the null voltage to be aligned with Q point as illustrated in Fig. 3. When the electric voltage, which has an arbitrary waveform such as a toneburst signal as shown in Fig. 3, is applied to an EOM, the laser intensity is proportionally modulated to the shape of the input electric voltage. Thus, an arbitrary light waveform can be produced to remotely excite a PZT transducer.

2.3 Conversion to electric signals using a photodiode

In order to excite a PZT transducer via a laser, it is necessary to convert the modulated optical power (intensity) into an electric signal. In this study, a photodiode made of a *pn* junction is used for this conversion due to its small size, high conversion speed, and good sensitivity. The photodiode generates a current flow (photocurrent) in an external circuit. The greater the light intensity is, the higher and larger the photogeneration rate and the photocurrent (I_{ph}) become. The photocurrent, I_{ph} , is linearly proportional to the incident optical intensity, P (Kasap 2001)

$$I_{ph} = kP \tag{2}$$

where k is a device-dependent constant.

An equivalent circuit of the photodiode is shown in Fig. 4 (Wilson and Hawkes 1998). In the figure, I_{ph} , I_D , I_p , R_p , R_s , R_L are the photocurrent, the diode current, the parallel resistance current, the parallel resistance, the series resistance and the external load, respectively. From the equivalent circuit analysis, the total current, I_L , becomes

$$I_L = -I_{ph} + I_D + I_p \tag{3}$$

In the above relationship, I_D is produced by the *pn* junction diode, and its behavior is governed by a typical diode characteristic

$$I_D = I_o \left[\exp\left(\frac{eV_L}{nk_B T}\right) - 1 \right] \tag{4}$$

where I_o is the reverse saturation current, e is an electron charge (-1.60×10^{-19} C), k_B is Boltzmann's constant ($8.61 \mu\text{eV/K}$), T is the absolute temperature of the photodiode and n is the ideality factor that depends on the semiconductor material and fabrication characteristics ($n = 1-2$) (Kasap 2001). R_s and R_p are typically a few ohms (or lower) and higher than 10^6 ohm, respectively. Therefore, I_p becomes negligible.

Typical $I_L - V_L$ characteristic of a photodiode is shown in Fig. 5, where I_o , k_B , n and T are set to be $40 \mu\text{A}$, $8.61 \mu\text{eV/K}$, 1.48 and 300 K, respectively. It can be shown that the $I_L - V_L$ characteristic is identical to the normal *pn* junction diode characteristic except that the $I_L - V_L$ curve is shifted down

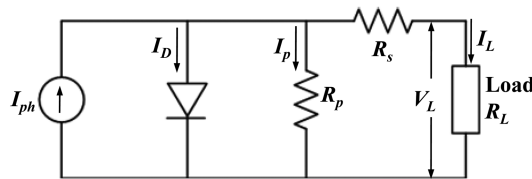


Fig. 4 An equivalent circuit model of a photodiode (Wilson and Hawkes 1998)

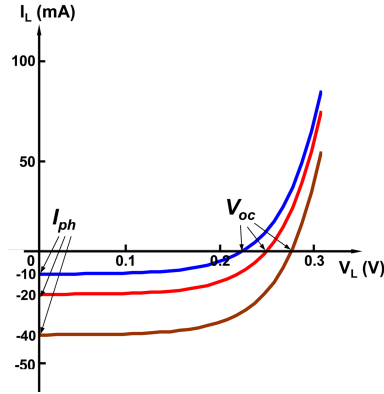


Fig. 5 A typical total current (I_L)- output voltage (V_L) characteristic of a photodiode based on Eqs. (3) and (4)

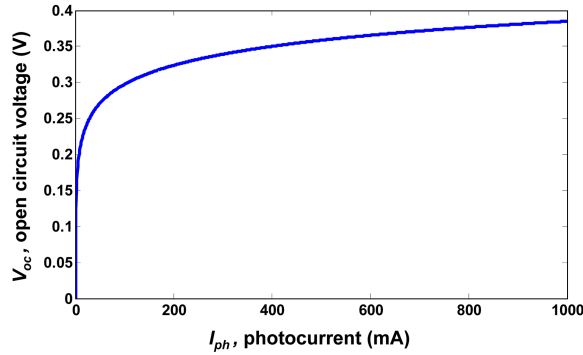


Fig. 6 The open circuit voltage (V_{oc}) of a photodiode as a function of the photocurrent (I_{ph}) in the range of 0 to 1000 mA based on Eq. (5)

by I_{ph} , which is linearly proportional to the light intensity. The open circuit output voltage, V_{oc} , of the photodiode is given by the point where the I_L - V_L curve intersects the V_L -axis ($I_L=0$) as

$$V_{oc} = \frac{nk_B T}{e} \ln\left(\frac{I_{ph}}{I_o} + 1\right) \quad (5)$$

Fig. 6 shows the relationship between I_{ph} and V_{oc} in the range of 0 to 1000 mA. It is apparent that the value of V_{oc} remains below 0.4 V even with a large photocurrent value of 1000 mA. Because this level of V_{oc} is not high enough to excite a typical PZT transducer used for guided wave generation, an additional step described in the next subsection is necessary before being able to excite the PZT properly.

2.4 Voltage amplification using a transformer

In the test configuration later described in the experiment, the PZT requires an input voltage of at least 1-2 V to generate measurable guided wave in the sensing PZT. However, because the photodiode in the previous step produces a voltage output below 0.4 V, a transformer is necessary for stepping up the voltage level of the converted electric signal. The transformer is an electromagnetic device designed to transfer electric energy with an increase or a decrease in voltage as shown in Fig. 7.

The ratio of the secondary induced voltage, V_2 , to the primary voltage, V_1 , is proportional to the ratio of the square root of inductances of their corresponding coils (Eq. (6)). Thus, the secondary induced voltage level can be adjusted by controlling the inductances ratio of these two coils.

$$\frac{V_2}{V_1} = \frac{\sqrt{L_2}}{\sqrt{L_1}}, \text{ if coupling coefficient} = 1 \text{ (an ideal transformer)} \tag{6}$$

3. Electrical circuit analysis

Electrical circuit analysis using PSPICE circuit analysis program (<http://www.cadence.com>) is conducted to verify the effect of a photodiode and a transformer on the input waveform applied to the PZT transducer. Fig. 7 shows the equivalent circuits of a photodiode, a transformer and a PZT transducer. The equivalent circuit model for the photodiode is previously presented in Fig. 4. An ideal transformer is assumed, resulting in a coupling coefficient of one. As for the PZT transducer, its impedance is modeled as RC circuit that predominantly has a capacitive behavior with a parallel resistive component (Georgiou and Mrad 2004).

For the circuit analysis of the PZT transducer node, the PZT has been modeled with the capacitance value, C_{PZT} , of 4.7 nF and the resistance value, R_{PZT} , of 450 Ω . Other parameters in Fig. 7 are $R_p = 1 \text{ M}\Omega$, $R_s = 1 \Omega$, $L_1 = 0.075 \text{ mH}$ and $L_2 = 1.07 \text{ mH}$. To model the *pn* junction diode, I_o , k_B , n and T are set to same parameters values used in Fig. 5. Those parameters were measured using a conventional digital multimeter (F87-5, Fluke. Inc.). I_{ph} generated by the laser source has a toneburst waveform in Eq. (7) with a mean value of 29.19 mA, an amplitude of $\pm 12.08 \text{ mA}$, and a driving frequency of 150 kHz as shown in Fig. 8. Note that these values of design parameters are chosen in accordance with the experiments presented in section 4.

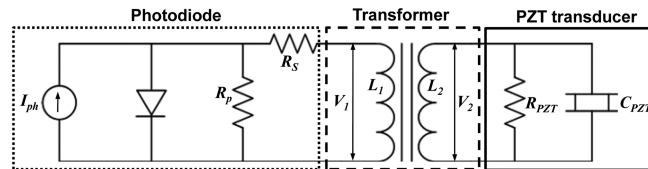


Fig. 7 An equivalent circuit of a PZT transducer node for wireless guided wave generation

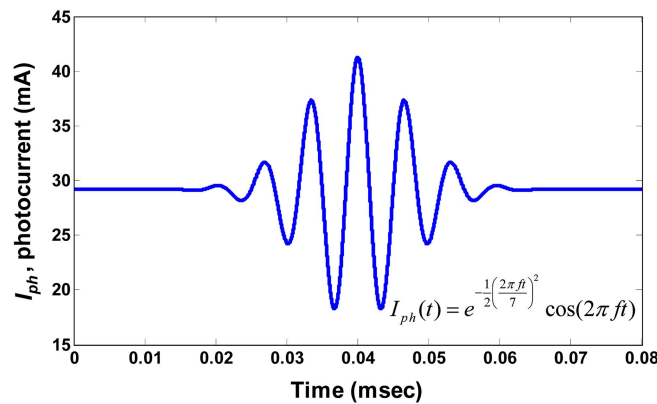


Fig. 8 A toneburst input photocurrent (I_{ph}) based on Eq. (7)

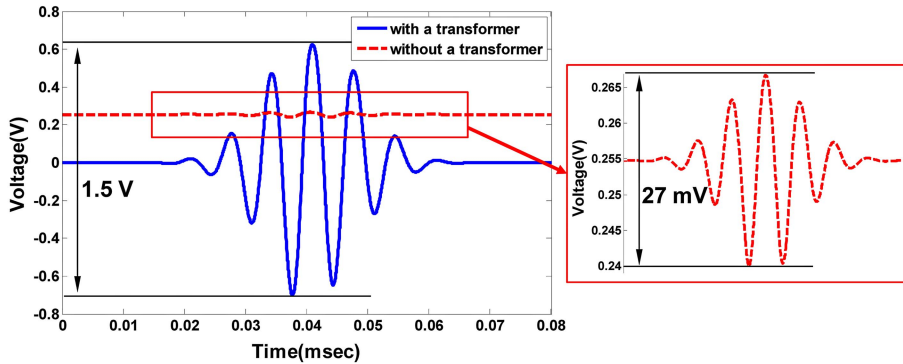


Fig. 9 Output voltage generated from a photodiode and applied to the exciting PZT with or without passing through the transformer

$$I_{ph}(t) = e^{-\frac{1}{2}\left(\frac{2\pi ft}{7}\right)^2} \cos(2\pi ft) \tag{7}$$

where f is a driving frequency.

Fig. 9 shows the output voltages generated from the photodiode and applied to the exciting PZT with or without going through the transformer. The voltage without the transformer (a dashed line) has about 255 mV offset, and the peak-to-peak amplitude of the toneburst component is only 27 mV. As expected, the voltage level is not high enough to excite the PZT transducer. On the other hand, the output voltage with the transformer (a solid line) is amplified up to the peak-to-peak amplitude of 1.5 V and this voltage level is enough to excite the PZT transducer. Note that the transformer also acts as a high pass filter and removes the unnecessary DC component.

Besides the voltage level, other issues of concern are phase distortion and time delay of the output voltage. As shown in Fig. 10, both output toneburst waveforms generated with or without passing through the transformer are distorted compared to the waveform of I_{ph} . Also, output voltage is delayed $0.61 \mu s$ during conversion to electric signal at the photodiode. It is speculated that the delay is mainly attributed to the diode characteristics because it takes time for electrons and holes to drift

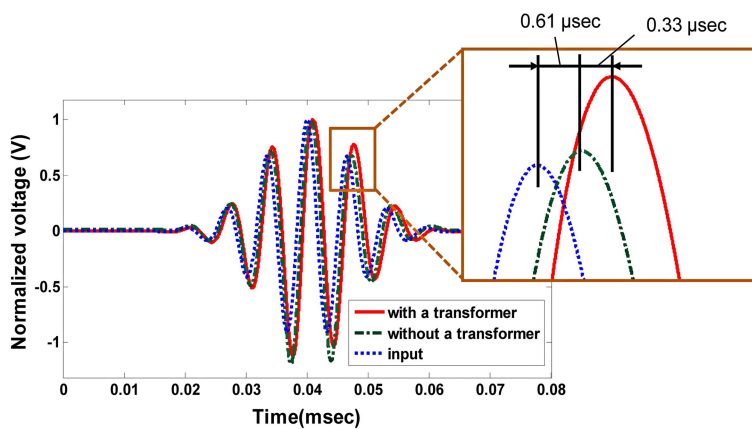


Fig. 10 Phase distortion and time delay of the output voltages with or without passing through the transformer

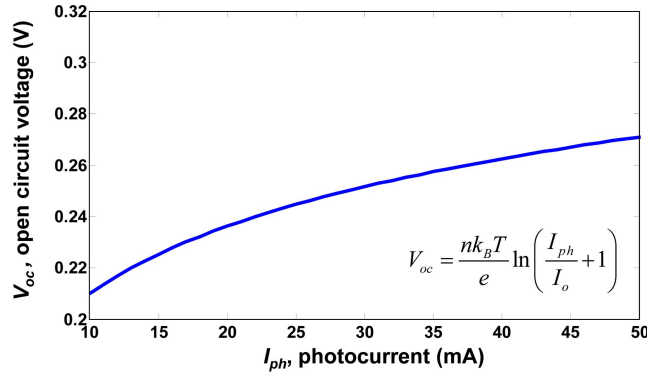


Fig. 11 A nonlinear relationship between I_{ph} and V_{oc} in the range of 10 mA to 50 mA based on Eq. (5)

in opposite directions to generate a photocurrent (Wilson and Hawkes 1998). In addition, output voltage is delayed $0.33 \mu s$ during voltage amplification at the transformer. For a better comparison, each signal is normalized with respect to its maximum value. It is speculated that the characteristics of a photodiode and a transformer attribute to the distortion and delay of the waveform. Fig. 11 shows the relationship between I_{ph} and V_{oc} of the photodiode in the operational range of 10 mA to 50 mA. As described in Eq. (5), the photodiode has a typical nonlinear relation between I_{ph} and V_{oc} . In addition, the transformer, which amplifies the voltage level through inductive coupling between two coils, intrinsically has resistance and capacitance components. These also contribute to the delay and phase distortion of the input signal. Those effects are explored experimentally in the following section.

Fig. 12 shows the amplitude of the output voltage generated from the photodiode with the transformer as a function of the driving frequency and the level of I_{ph} . The interaction between the inductance (L_2) of the transformer and the capacitance (C_{PZT}) of the PZT results in a resonance phenomenon. Here, the resonance frequency can be approximated as follows (Greve *et al.* 2007)

$$f = \frac{1}{2\pi\sqrt{L_2 C_{PZT}}} \text{ (Hz)} \tag{8}$$

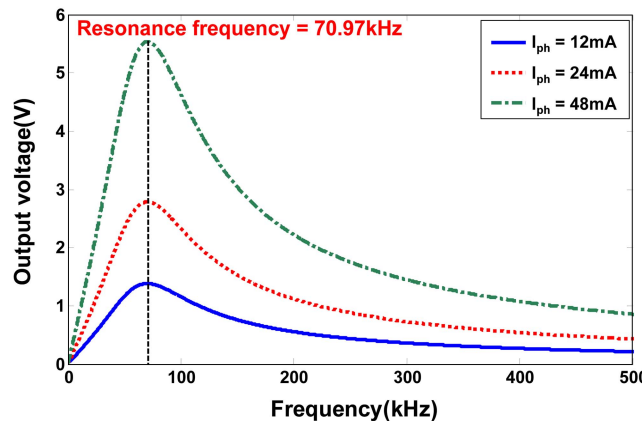


Fig. 12 The relationship of the output voltage at the PZT transducer node with the driving frequency and the level of I_{ph}

From the circuit model in Fig. 7, the theoretical resonance frequency is calculated to be 70.97 kHz ($L_2 = 1.07$ mH, $C_{PZT} = 4.7$ nF). As expected, the analysis result shows a good agreement with theoretical one. Next, three different amplitudes (12 mA, 24 mA and 48 mA) of I_{ph} are applied to the circuit to verify the relationship between I_{ph} and the output voltage. The output voltage increases in proportion to the input I_{ph} . Note that, from a mechanical point of view, the actual amplitude of the guided waves generated at the exciting PZT is also influenced by the interaction between the size and shape of a PZT transducer and the driving frequency (Sohn *et al.* 2010). For instance, when the wavelength of a specific guided wave mode becomes twice of a PZT transducer size, the amplitude of that particular mode is amplified. Therefore, not only parameters of electronic components such as L_1 , L_2 , I_{ph} and C_{PZT} but also the driving frequency and the PZT configuration have to be optimized to maximize the magnitude of the output voltage and guided waves.

4. Experimental characterization

4.1 Experimental setup

To examine the proposed optical technique for wireless guided wave generation, experimental tests were conducted. The overall test configuration and the test specimen are shown in Fig. 13. The system was composed of a laser diode as a power source, an EOM and an arbitrary waveform generator (AWG) for intensity modulation of the laser, an optical amplifier, a collimator, a photodiode, a transformer and PZT transducers attached on an aluminum specimen.

The dimensions of the specimen and the PZT transducer node are shown in Fig. 14. The dimensions of the aluminum plate used in this study were 610 mm \times 400 mm \times 6 mm and two PSI-5AE type capsulated PZT wafer transducers (PZTs A and B) were mounted on the aluminum plate. The radius of each PZT was 9 mm and its thickness was 0.508 mm. The excitation PZT node (PZT A) consists of a PZT transducer and an integrated photodiode and transformer component connected through an SMA (SubMiniature version A, 1979) connector. PZT B was placed 0.290 m apart from PZT A. Note that PZTs A and B were both connected to the oscilloscope using BNC cables to record the guided wave response signals.

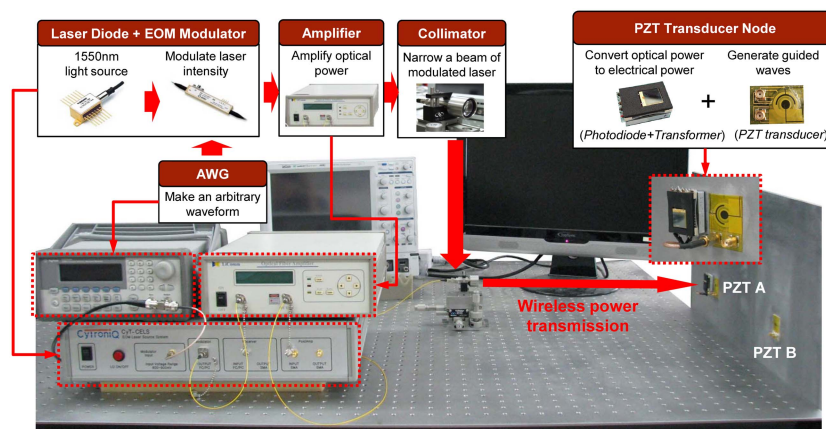


Fig. 13 An overall experimental setup of the proposed wireless guided wave excitation system

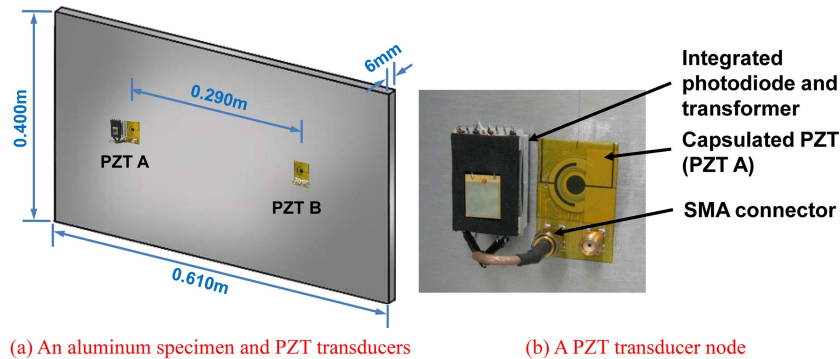


Fig. 14 An aluminum specimen, a PZT transducer node (PZT A) for guided wave excitation and another PZT transducer (PZT B) for guided wave sensing

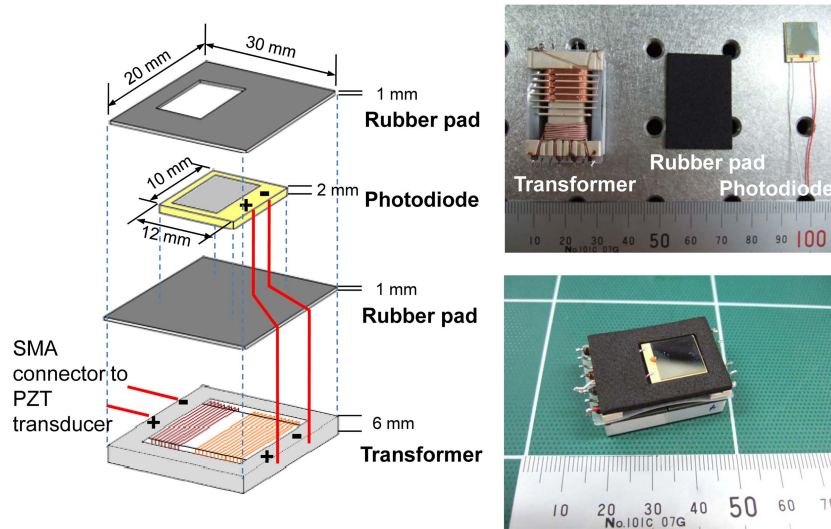


Fig. 15 Design of an integrated photodiode and transformer component as part of the PZT transducer node for wireless guided wave generation

Fig. 15 shows a specific design of a self-sufficient PZT transducer node combined with a photodiode and a transformer. A commercial photodiode (FDG1010, Thorlab Inc.) was used, and the internal parameters of each component were same as those used in the previous electrical circuit analysis. The rubber pads were used to prevent electrical interference between the photodiode and the transformer and to protect them, and the integrated photodiode and transformer was connected to a PZT transducer through an SMA connector. When the laser is focused on the photodiode, the node converts the light into an electric signal, amplifies the voltage, and generates guided waves on a structure by exciting the PZT. Thus, it does not need any power source or a signal generator at the PZT transducer node.

The output power of the laser diode used in this experiment was 10 mW and controlled by the laser driver. Using the AWG, a toneburst signal with 2 V peak-to-peak voltage was generated at a driving frequency of 150 kHz and exerted to the EOM for intensity modulation of the laser. This modulated laser power was amplified up to 80 mW by the optical amplifier and transmitted by

optical fiber to the collimator. The collimated laser was emitted into air and aimed at the integrated photodiode and transformer for conversion to an electric signal and amplification of voltage level. Then, PZT A generated guided waves, and the responses were measured at both PZTs A and B. PZT A was also excited by using conventional wire connection to the AWG, and the corresponding responses were measured at PZTs A and B. The response data were collected using a conventional oscilloscope (WaveRunner44Xi, LeCroy. Inc.). The sampling rate and resolution of the oscilloscope were 100 MHz and 8 bits, respectively. In order to improve the signal-to noise ratio, the responses were measured 20 times and averaged in the time domain.

Several aspects of the proposed wireless power transmission system were investigated. First, the waveform of the generated electric signal at the PZT transducer node was compared to the original input signal by checking phase distortion and time delay as well as amplitude and frequency. Then, the power transmission efficiencies at each device were evaluated quantitatively. Also, the distance between the laser and the PZT transducer node was gradually increased up to 5 m to examine the change of the energy transmission efficiency. Finally, the guided waves measured from wired and wireless systems were compared for verification of the performance of the proposed system. Detailed test results are presented in the next sub-sections.

4.2 Verification of the input waveform

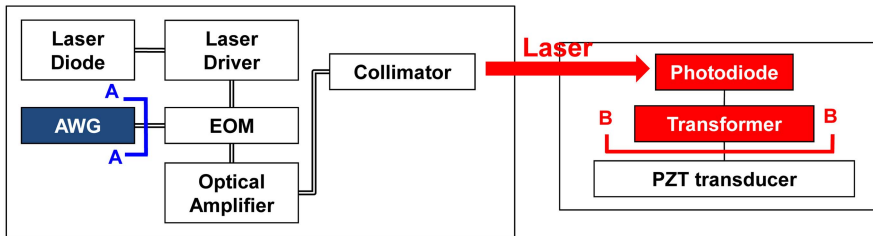
Fig. 16 compares the toneburst waveforms generated by a laser and an AWG. In Fig. 16(a), the input toneburst signals are measured at two points: Signal AA is a toneburst signal generated by the AWG and measured at A-A point, and signal BB is the one measured at B-B point after the toneburst input goes through the photodiode and the transformer.

Signal AA is shown as a dotted line in Fig. 16(b). Its peak-to-peak voltage and the driving frequency were 2 V and 150 kHz, respectively. Subsequently signal BB was delineated by a solid line, and the peak-to-peak voltage and the driving frequency of the output signal were 1.41 V and 150 kHz, respectively. There was about 1.59 μ s time delay between these two toneburst signals.

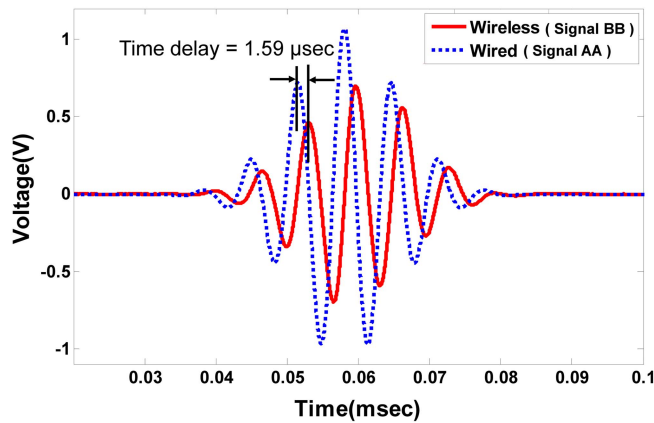
To compare only the shapes of these two signals, each signal was normalized with respect to its maximum value, and signal BB was shifted in time to be aligned with signal AA as shown in Fig. 16(c). Fig. 16(c) shows a fairly good agreement of these signals' waveforms. However, there was a small distortion of signal BB's waveform with respect to signal AA. The finding here is consistent with the electrical circuit analysis shown in Fig. 10. Note that both the photodiode and the transformer have intrinsic nonlinear characteristics and the transfer function of the EOM in the range of $0-V_{\pi}$ is not exactly linear as Eq. (1). It is speculated that these nonlinear characteristics contributed to the signal distortion. The development of a calibration technique is underway by the authors to compensate the signal distortion using the empirical transfer function of the system (Lee *et al.* 2009).

4.3 Investigation of the power transmission efficiency

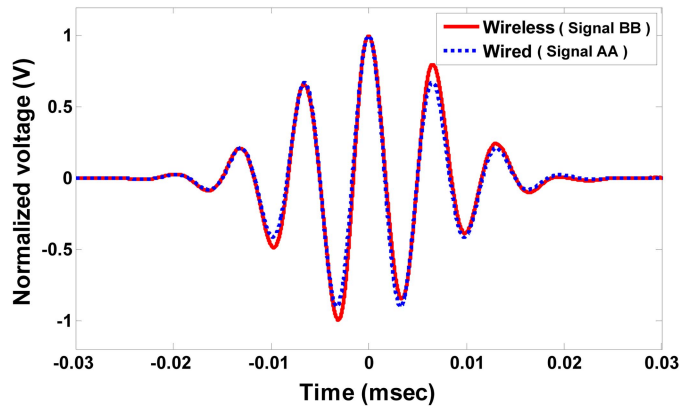
Here, the power transmission efficiencies at each device were evaluated quantitatively. Fig. 17 shows optical and electric power measured at each device level. The optical power and the electric power were measured using a conventional optical power meter (PM100D, Thorlab.Inc.) and an oscilloscope (WaveRunner44Xi, LeCroy. Inc.), respectively. As mentioned in the previous section, a 10 mW laser diode was used as a power source. The power level was decreased to 3.42 mW during



(a) Measurement of the input waveform: signals AA and BB are measured at A-A and B-B points



(b) Comparison of signals AA and BB before normalization



(c) Comparison of signals AA and BB after normalization

Fig. 16 Comparison of the input toneburst signals generated by a laser and an AWG

the modulation process and then amplified about 20 times using the optical amplifier. Consequently the optical power measured at the PZT transducer node was 56.7 mW and it was converted into 7.30 mW of electrical power. From the results, it has been found that the power transmission efficiency in the wireless power transmission was 12.87% on average. The transformer stepped up the voltage level of the converted 7.30 mW electric power and 1.41 V of output voltage was produced.

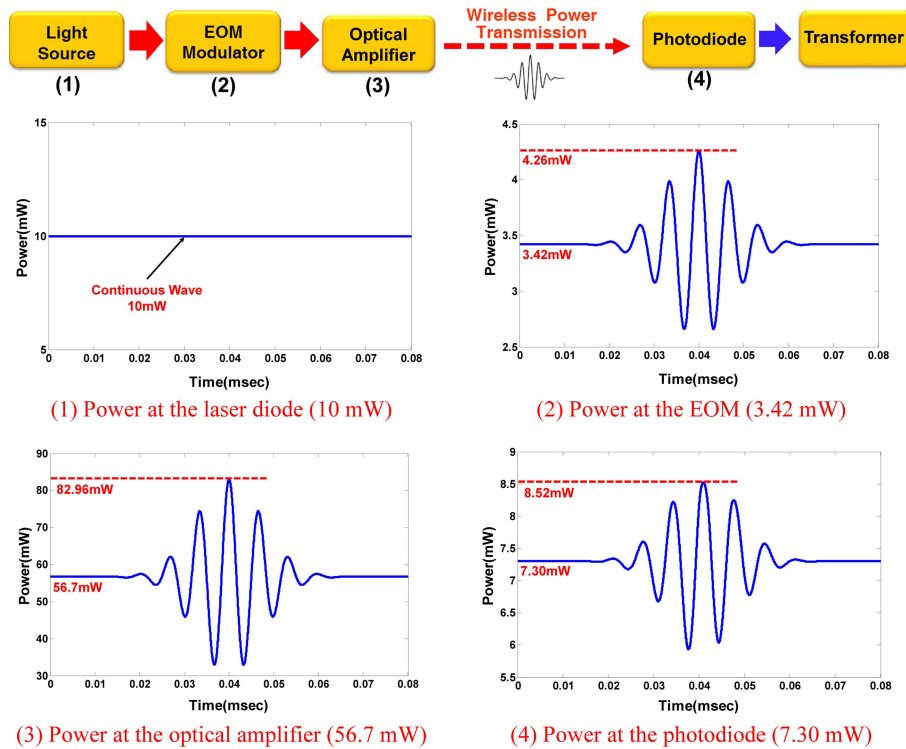


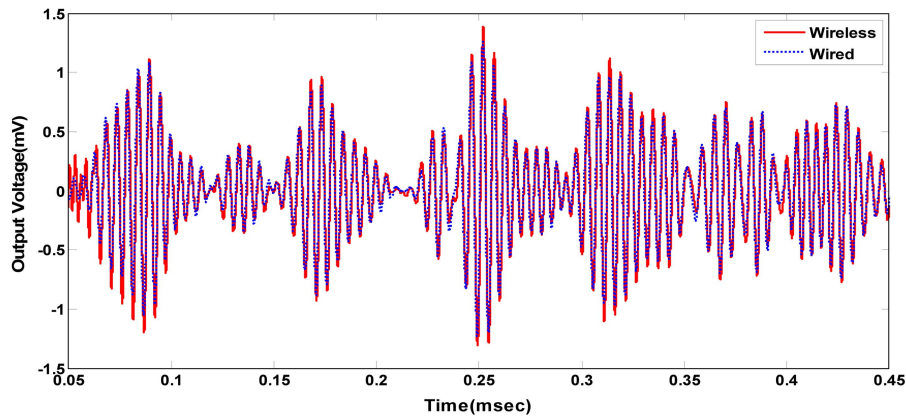
Fig. 17 Investigation of wireless power transmission efficiency: the power transmission efficiency in wireless power transmission was 12.87% regardless of the wireless power distances investigated in this study (up to 5 m)

4.4 Investigation of the wireless power transmission distance

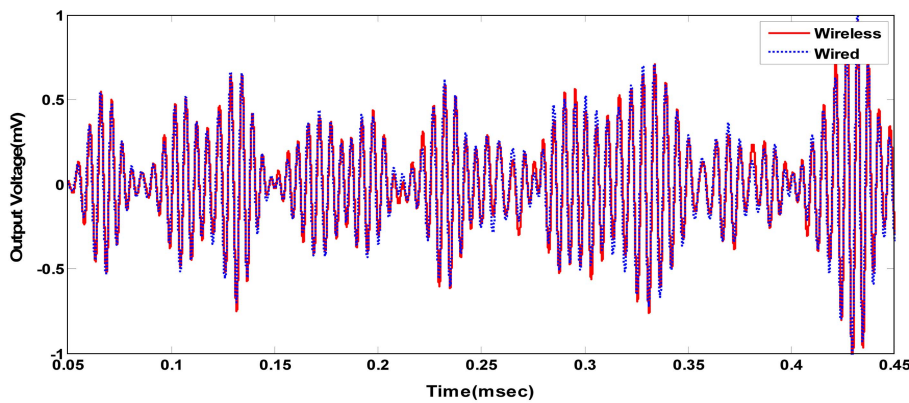
The distance between the laser and the PZT transducer node was then gradually increased up to 5 m to examine the change of the energy transmission rate with the distance. The maximum wireless power transmission distance here was limited by the size of the available optical table. At least up to the maximum distance investigated here, the power transmission efficiency was not affected by the distance between the laser source system and the PZT transducer node. Using the collimator, the divergence of the laser was minimized and the spot size of the laser beam focused on the photodiode was controlled to be about 0.12 mm^2 for all transmission distances investigated here. However, the actual power transmission efficiency might be reduced in field due to varying environmental and operational conditions such as foggy weather and misalignment of the laser beam. A further study is underway to develop a control system that can precisely aim the laser source to the target PZT even when the target is moving.

4.5 Comparison of the guided waves generated by wired & wireless systems

Fig. 18 shows the guided waves measured at PZTs A and B when PZT A was excited with wired and wireless systems, respectively. As for the wireless system, the modulated laser remotely excited PZT A, and the corresponding guided wave responses were measured at PZTs A and B, respectively.



(a) Guided waves measured at PZT A



(b) Guided waves measured at PZT B

Fig. 18 Comparison of the guided waves generated by wired and wireless systems

In the wired system, PZT A was excited this time by using a conventional wire connection to the AWG and the responses were measured in the same way as the wireless system. Each signal was divided by its standard deviation value before comparison. Fig. 18(a) shows that the guided waves generated by the wireless system and measured at PZT A were very similar to the corresponding responses created by the wired system. A similar result was found for the responses measured at PZT B in Fig. 18(b). This comparison with the conventional wired generation method confirms that the laser-based technique can properly generate guided waves.

5. Conclusions

A new wireless guided wave system based on laser and optoelectronic technology is proposed so that power as well as data for PZT excitation and sensing can be transmitted via a laser. The present work focuses mainly on the excitation aspect of the system. First, a laser is used as a power source and an arbitrary waveform such as a toneburst signal is generated using an electro-optic modulator (EOM). The modulated laser is amplified by an optical amplifier and emitted to a photodiode. The

photodiode converts the light into an electric signal, and a transformer increases the voltage level of the converted electric signal. Finally, this electric voltage is used to excite a PZT transducer and guided waves are generated in the structure where the PZT is attached. The feasibility of the power transmission aspect of the proposed wireless scheme has been experimentally demonstrated in a laboratory setup. The experimental results demonstrated that the laser-based guided wave generation technique can wirelessly excite a PZT transducer and produce measurable guided waves in a thin aluminum plate with an overall power transmission efficient of 12.87%. Using the proposed technology, a PZT transducer can be permanently attached to a structure without requiring complex electronic components, wired power supply or onboard batteries, making it possible to develop a self-contained, rugged and non-intrusive PZT node. A further research for wireless guided wave sensing is currently being developed by the authors using other optoelectronic devices, such as photovoltaic panels and laser diodes (Park *et al.* 2010). Finally, it is envisioned that the developed technology can be integrated with autonomous moving agents such as robots to remotely inspect the integrity and performance of large distributed infrastructure systems such as bridges.

Acknowledgements

This work was supported by the Radiation Technology Program (M20703000015-07N0300-01510), the Nuclear Research & Development Program (2009-0083489), and the Basic Science Research Program (NRF 2007-314-D00032) of National Research Foundation of Korea (NRF) funded by Ministry of Education, Science & Technology (MEST).

References

- Achenbach, J.D. (2000), "Quantitative nondestructive evaluation", *Int. J. Solids Struct.*, **37**, 13-27.
- Castainings, M. and Hosten, B. (2001), "Lamb and SH waves generated and detected by air-coupled ultrasonic transducers in composite material plates", *NDT & E Int.*, **34**, 249-258.
- Çelebi, M. (2002), *Seismic instrumentation of buildings (with emphasis of federal buildings)*, Technical report No. 0-7460-68170.
- Clark, M., Linnane, F., Sharples, S.D. and Somekh, M.G. (1998), "Frequency control in laser ultrasound with computer generated holography", *Appl. Phys. Lett.*, **72**(16), 1963-1965.
- Georgiou, H.M.S. and Mrad, R.B. (2004), "Experimental and theoretical assessment of PZT modeled as RC circuit subject to variable voltage excitations", *Mechatronics*, **14**(6), 667-674.
- Ghosh, T., Kundu, T. and Karpur, P. (1998), "Efficient use of Lamb modes for detecting defects in large plates", *Ultrasonics*, **36**, 791-801.
- Giurgiutiu, V. (2008), *Structural Health Monitoring with Piezoelectric Wafer Active Sensors*, Elsevier Inc., London.
- Greve, D.W., Sohn, H., Yue, C.P. and Oppenheim, I.J. (2007), "An Inductively coupled lamb wave transducer", *IEEE Sens. J.*, **7**(2), 295-301.
- Grisso, B.L. and Inman, D.J. (2008), "Autonomous hardware development for impedance-based health monitoring", *Smart Struct. Syst.*, **4**(3), 305-318.
- Guo, N. and Cawley, P. (1994), "Lamb wave reflection for the quick nondestructive evaluation of large composite laminates", *Mater. Eval.*, **52**, 404-411.
- Guo, Z., Achenbach, J.D. and Krishnaswamy, S. (1997), "EMAT generation and laser detection of single Lamb wave modes", *Ultrasonics*, **35**(6), 423-429.
- Kasap, S.O. (2001), *Optoelectronics and Photonics: Principles and Practices*, Prentice Hall, New Jersey.
- Khare, R.P. (2004), *Fiber Optics and Optoelectronics*, Oxford University Press, India.

- Kim, S.B. and Sohn, H. (2007), "Instantaneous reference-free crack detection based on polarization characteristics of piezoelectric materials", *Smart Mater. Struct.*, **16**(6), 2375-2387.
- Lee, H.S., Park, H.J., Sohn, H. and Kwon, I.B. (2009), "A Hybrid PZT/FBG guided wave generation and sensing system using a single laser source", *Proceedings of the International Conference on Computational Design in Engineering*, Seoul, Korea, November.
- Lu, K.C., Loh, C.H., Yang, Y.S., Lynch, J.P. and Law, K.H. (2008), "Real-time structural damage detection using wireless sensing and monitoring system", *Smart Struct. Syst.*, **4**(6), 759-777.
- Lynch, J.P. and Loh, K.J. (2006), "A summary review of wireless sensors and sensor networks for structural health monitoring", *Shock Vib. Digest*, **38**(2), 91-128.
- Mascarenas, D.L., Todd, M.D., Park, G. and Farrar, C.R. (2007), "Development of an impedance-based wireless sensor node for structural health monitoring", *Smart Mater. Struct.*, **16**(6), 2137-2145.
- Moulin, E., Assaad, J., Delebarre, C., Kaczmarek, H. and Balageas, D. (1997), "Piezoelectric transducer embedded in a composite plate: application to Lamb wave generation", *J. Appl. Phys.*, **82**(5), 2049-2055.
- Park, H.J., Sohn, H., Yun, C.B., Chung, J. (2010), "Wireless guided wave-based monitoring using laser based actuation and sensing", *Proceedings of the 6th Computational Stochastic Mechanics Conference*, Rhodos, Greece, June.
- RF Connectors (1979), *Radio-frequency connectors, Part 15: R.F. coaxial connectors with inner diameter of outer conductor 4.13 mm (0.163 in) with screw coupling - Characteristic impedance 50 ohms (Type SMA)*, International Electrotechnical Commission.
- Raghavan, A. and Cesnik, E.S. (2007), "Review of guided-wave structural health monitoring", *Shock Vib. Digest*, **39**(2), 91-114.
- Scruby, C.B. and Drain, L.E. (1990), *Laser Ultrasonics: Techniques and Applications*, Taylor & Francis Group, New York.
- Smith, S.D. (1995), *Optoelectronic Devices*, Prentice Hall, New Jersey.
- Sohn, H. (2003), "Active sensing based structural health monitoring for flaw detection in composite structures", *KSCE J. Civ. Eng.*, **7**(6), 637-646.
- Sohn, H., Park, G., Wait, J.R., Limback, N.P. and Farrar, C.R. (2004), "Wavelet-based active sensing for delamination detection in composite structures", *Smart Mater. Struct.*, **13**, 153-160.
- Sohn, H. and Lee, S.J. (2010), "Lamb wave tuning curve calibration for surface-bonded piezoelectric transducers", *Smart Mater. Struct.*, **19**, 1-12.
- Su, Z., Ye, L. and Lu, Y. (2006), "Guided Lamb waves for identification of damage in composite structures: a review", *J. Sound Vib.*, **295**, 753-780.
- Svelto, O. (1982), *Principles of Lasers*, Plenum, New York.
- Wang, L. and Yuan, F.G. (2007), "Active damage localization technique based on energy propagation of Lamb waves", *Smart Struct. Syst.*, **3**(2), 201-217.
- Wilson, J. and Hawkes, J. (1998), *Optoelectronics: An introduction*, Prentice Hall, New Jersey
- Yeatman, E.M. (2009), "Energy harvesting-small scale energy production from ambient sources", *Proceedings of the SPIE, the International Society for Optical Engineering*, San Diego CA, USA, March.